

Reactions of an antimony containing cage compound with metal carbonyls: synthesis and structural characterization of $[\{M(CO)_5\}_2(\eta^1:\eta^1-P_4Sb_2C_4Bu^t_4)]$, $M = Cr, Mo$ or W , and $[\{Fe(CO)_4\}_2\{Fe(CO)_3(\eta^3:\eta^1-P_4Sb_2C_4Bu^t_4)\}]$

David E. Hibbs, Michael B. Hursthouse, Cameron Jones* and Ryan C. Thomas

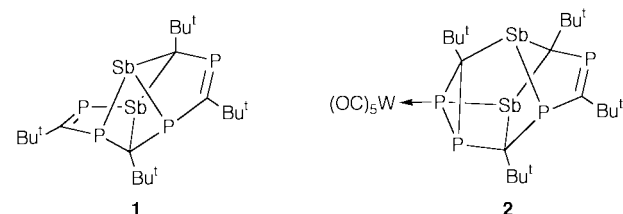
Department of Chemistry, University of Wales, Cardiff, P.O. Box 912, Park Place, Cardiff, UK CF1 3TB

Received 20th April 1999, Accepted 23rd June 1999

The antimony containing cage compound, $P_4Sb_2C_4Bu^t_4$, was treated with an excess of $[M(CO)_5(THF)]$, $M = Cr, Mo$ or W , to produce the 2:1 adduct complexes, $[\{M(CO)_5\}_2(\eta^1:\eta^1-P_4Sb_2C_4Bu^t_4)]$, which X-ray crystallographic studies have shown to contain one $M(CO)_5$ fragment co-ordinated to an unsaturated phosphorus centre and one co-ordinated to an antimony centre. In contrast, its reaction with an excess of $[Fe_2(CO)_9]$ produced $[\{Fe(CO)_4\}_2\{Fe(CO)_3(\eta^3:\eta^1-P_4Sb_2C_4Bu^t_4)\}]$, which is probably formed by the insertion of an $Fe(CO)_3$ fragment into an Sb–P bond of the cage. Its crystal structure confirms that it contains two η^1 -co-ordinated $Fe(CO)_4$ groups and a 1,3-diphosphaallyl fragment η^3 co-ordinated to an $Fe(CO)_3$ moiety.

Introduction

In recent years there has been a considerable amount of attention paid to the chemistry of organophosphorus cage compounds as they show remarkable similarities to their hydrocarbon cage analogues.¹ One difference between the two is the ability of organophosphorus cages to act as ligands through P-lone pair donation, a feature that has been widely exploited.² Although not as widely studied as organophosphorus cages, cage compounds containing organo-arsenic or -antimony fragments are known and their interaction with transition metal complexes, especially in the preparation of Group 15–transition metal cluster compounds, has been investigated.³ We have recently added to this area with the synthesis of the mixed P,Sb-substituted cage compound **1**, which is prepared in high



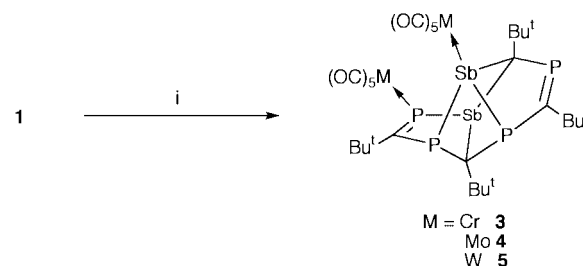
yield *via* the oxidative coupling of two equivalents of the diphosphastibolyl ring anion $[1,4,2-P_2SbC_2Bu^t_2]^-$ with $FeCl_3$.⁴

Compound **1** offers many potential sites for metal fragment co-ordination, either through P- or Sb-lone pair donation or η^2 co-ordination to its P–C double bonds. Previously, we have found that the reaction of **1** with $[W(CO)_5(THF)]$ did not lead to the formation of an adduct but to a low yield (9%) of **2** which presumably forms *via* a metal mediated rearrangement reaction.⁵ In this earlier study no other product could be isolated from the reaction mixture. We have since discovered that a simple adduct can form from this reaction in addition to those involving $[Cr(CO)_5(THF)]$ and $[Mo(CO)_5(THF)]$. We have also investigated the interaction of **1** with $[Fe_2(CO)_9]$ and other metal carbonyls. The results of these investigations are reported herein.

Results and discussion

The reaction of compound **1** with 2 equivalents of $[M(CO)_5-$

$(THF)]$, $M = Cr, Mo$ or W , led to the formation of the isostructural 2:1 adducts, **3–5**, in moderate yields (24, 29 and 27% respectively) (Scheme 1). There was no evidence for the form-



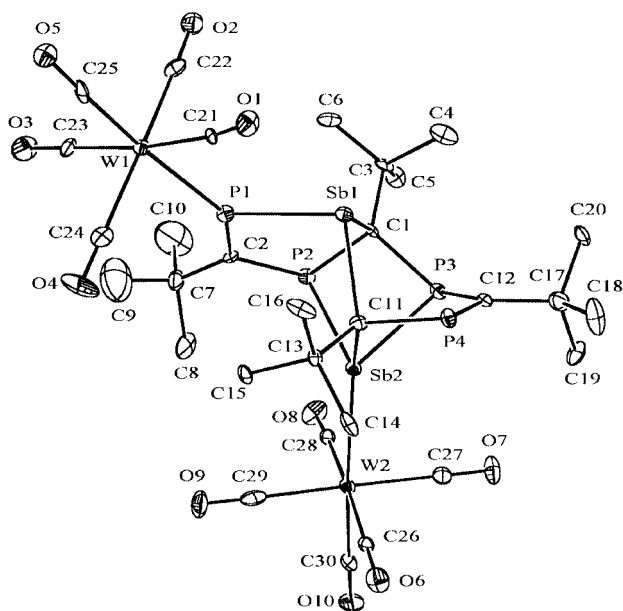
Scheme 1 Reagents and conditions: i, $[W(CO)_5(THF)]$, THF, 18 h.

ation of higher adducts but a small amount of the previously reported rearrangement product, **2**, was observed in the preparation of **5**. In contrast there was no indication that the chromium or molybdenum analogues of **2** were formed in the preparation of **3** or **4**. Efforts to identify the products other than **3–5** from these reactions proved unsuccessful but ^{31}P NMR studies suggested a complex mixture of intractable by-products that did not contain the unco-ordinated cage, **1**. Moreover, changing the reaction times for the preparations of **3–5** did not significantly effect their yields. It is thought that no trace of **5** was seen in the previously reported preparation of **2** because in that case the product mixture was purified by column chromatography (Kieselgel/hexane) and we have found that **5** is not stable to these chromatographic conditions. Interestingly, **3** and **4** can be chromatographed but do show signs of partial decomposition when this is attempted.

The solution $^{31}P\{-^1H\}$ NMR spectra of compounds **3–5** are similar and support their proposed structures. In the case of **5** the spectral pattern is consistent with an AMNX spin system and displays four inequivalent phosphorus resonances, two at low field [$P(4) \delta 346.2$, $P(1) 268.5$] in the normal phosphalkene region⁶ and two at higher field [$P(3) \delta 43.6$, $P(2) -32.0$] in the saturated phosphorus region (NB: numbering scheme is taken from Fig. 1). All These resonances are close to those seen for the unco-ordinated cage, **1**, with the exception of that for $P(1)$ which is shifted to higher field by *ca.* 95 ppm which strongly

Table 1 Selected intramolecular distances (Å) and angles (°) for compound **3** with estimated standard deviations (e.s.d.s) in parentheses

Cr(1)–P(1)	2.387(3)	Cr(2)–Sb(2)	2.6290(14)
Sb(1)–C(1)	2.171(7)	C(12)–C(17)	1.578(10)
Sb(1)–C(11)	2.236(7)	Sb(1)–P(1)	2.530(2)
Sb(2)–C(11)	2.211(9)	Sb(2)–P(3)	2.500(2)
Sb(2)–P(2)	2.520(2)	P(1)–C(2)	1.684(8)
P(2)–C(2)	1.790(8)	P(2)–C(1)	1.890(7)
P(3)–C(12)	1.863(8)	P(3)–C(1)	1.925(8)
P(4)–C(12)	1.662(8)	P(4)–C(11)	1.835(8)
C(1)–C(3)	1.606(10)	C(2)–C(7)	1.602(10)
C(11)–C(13)	1.556(10)	C(12)–C(17)	1.589(10)
C(1)–Sb(1)–C(11)	89.5(3)	C(1)–Sb(1)–P(1)	89.8(2)
C(11)–Sb(1)–P(1)	100.3(2)	C(11)–Sb(2)–P(3)	84.7(2)
C(11)–Sb(2)–P(2)	97.8(2)	P(3)–Sb(2)–P(2)	70.11(7)
C(11)–Sb(2)–Cr(2)	137.9(2)	P(3)–Sb(2)–Cr(2)	122.21(6)
P(2)–Sb(2)–Cr(2)	120.59(6)	C(2)–P(1)–Cr(1)	141.4(3)
C(2)–P(1)–Sb(1)	100.3(3)	Cr(1)–P(1)–Sb(1)	118.01(10)
C(2)–P(2)–C(1)	108.0(4)	C(2)–P(2)–Sb(2)	107.0(3)
C(1)–P(2)–Sb(2)	83.1(3)	C(12)–P(3)–C(1)	108.0(3)
C(12)–P(3)–Sb(2)	92.8(2)	C(1)–P(3)–Sb(2)	83.0(2)
C(12)–P(4)–C(11)	104.9(4)	C(3)–C(1)–P(2)	113.1(5)
C(3)–C(1)–P(3)	113.8(5)	P(2)–C(1)–P(3)	98.2(3)
C(3)–C(1)–Sb(1)	111.4(5)	P(2)–C(1)–Sb(1)	107.5(3)
P(3)–C(1)–Sb(1)	112.0(4)	C(7)–C(2)–P(1)	125.4(6)
C(7)–C(2)–P(2)	111.7(6)	P(1)–C(2)–P(2)	122.9(4)
C(13)–C(11)–P(4)	114.9(6)	C(13)–C(11)–Sb(2)	114.7(5)
P(4)–C(11)–Sb(2)	107.3(4)	C(13)–C(11)–Sb(1)	115.5(5)
P(4)–C(11)–Sb(1)	95.5(3)	Sb(2)–C(11)–Sb(1)	107.0(3)
C(17)–C(12)–P(4)	120.6(6)	C(17)–C(12)–P(3)	114.9(6)
P(4)–C(12)–P(3)	124.0(4)		

**Fig. 1** Molecular structure of compound **5**.

suggests this is co-ordinated to a $W(CO)_5$ fragment. This is confirmed by the presence of tungsten satellites ($^1J_{WP} = 208.0$ Hz) about this signal. All the P–P couplings in the spectrum are normal apart from that between P(2) and P(3), ($^2J_{PP} = 147.5$ Hz), which is very large but compares well with the same coupling for **1** (137 Hz). This can, perhaps, be explained as a through space coupling which results from the short intermolecular P(2)–P(3) distance (see below). The only significant differences between the $^{31}P\{-^1H\}$ NMR spectra of **5** and those of **3** and **4** arises from the position of the P(1) resonance which in the cases of **4** (δ 307.7) and **3** (328.5) move closer to the equivalent resonance for the free cage, **1** (δ 363), as the molecular weight of the metal involved decreases. This phenomenon has been observed and explained on prior occasions for other phosphine– $M(CO)_5$, $M = Cr, Mo$ or W , adducts.⁷ The 1H NMR spectra for **3–5** are

Table 2 Selected intramolecular distances (Å) and angles (°) for compound **4** with e.s.d.s in parentheses

Sb(1)–C(1)	2.175(9)	Sb(1)–C(11)	2.203(9)
Sb(1)–P(1)	2.534(3)	Sb(2)–C(11)	2.211(9)
Sb(2)–P(3)	2.497(2)	Sb(2)–P(2)	2.517(3)
Sb(2)–Mo(2)	2.7593(13)	Mo(1)–P(1)	2.527(3)
P(1)–C(2)	1.741(12)	P(2)–C(2)	1.847(10)
P(2)–C(1)	1.866(10)	P(3)–C(12)	1.893(10)
P(4)–C(12)	1.683(9)	P(4)–C(11)	1.829(10)
C(1)–C(3)	1.603(12)	C(2)–C(7)	1.426(14)
C(11)–C(13)	1.583(11)	C(12)–C(17)	1.511(13)
P(3)–C(1)	1.946(10)		
C(1)–Sb(1)–C(11)	88.9(3)	C(1)–Sb(1)–P(1)	89.9(3)
C(11)–Sb(1)–P(1)	100.0(3)	C(11)–Sb(2)–P(3)	85.2(2)
C(11)–Sb(2)–P(2)	97.0(3)	P(3)–Sb(2)–P(2)	69.86(9)
C(11)–Sb(2)–Mo(2)	139.2(2)	P(3)–Sb(2)–Mo(2)	121.20(7)
P(2)–Sb(2)–Mo(2)	120.27(7)	C(2)–P(1)–Mo(1)	140.4(4)
C(2)–P(1)–Sb(1)	103.0(4)	Mo(1)–P(1)–Sb(1)	116.49(12)
C(2)–P(2)–C(1)	111.7(5)	C(2)–P(2)–Sb(2)	106.5(3)
C(1)–P(2)–Sb(2)	83.1(3)	C(12)–P(3)–C(1)	106.4(4)
C(12)–P(3)–Sb(2)	92.6(3)	C(1)–P(3)–Sb(2)	82.1(3)
C(12)–P(4)–C(11)	104.8(5)	P(2)–C(1)–P(3)	97.7(4)
C(3)–C(1)–Sb(1)	110.9(6)	P(2)–C(1)–Sb(1)	107.8(4)
P(3)–C(1)–Sb(1)	113.2(4)	P(1)–C(2)–P(2)	116.6(6)
P(4)–C(11)–Sb(1)	97.0(4)	P(4)–C(11)–Sb(2)	107.1(4)
Sb(1)–C(11)–Sb(2)	108.0(4)	P(4)–C(12)–P(3)	123.2(6)

Table 3 Selected intramolecular distances (Å) and angles (°) for compound **5** with e.s.d.s in parentheses

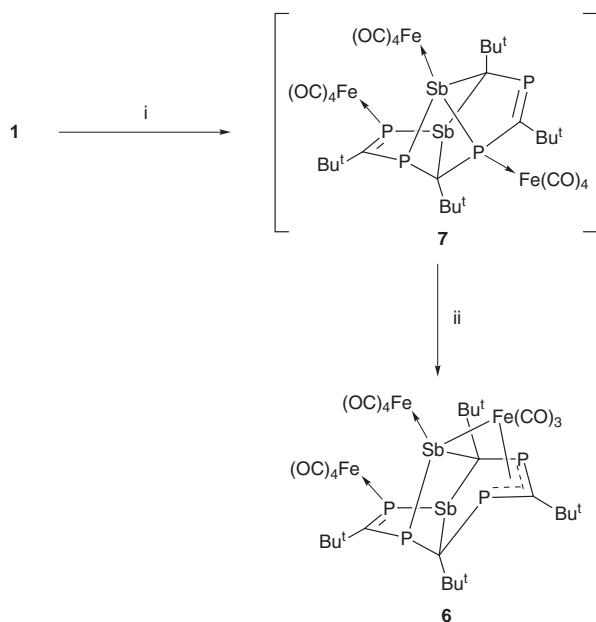
W(1)–P(1)	2.513(3)	W(2)–Sb(2)	2.7586(9)
Sb(1)–C(1)	2.196(10)	Sb(1)–C(11)	2.218(10)
Sb(1)–P(1)	2.521(3)	Sb(2)–C(11)	2.202(10)
Sb(2)–P(3)	2.499(3)	Sb(2)–P(2)	2.509(3)
P(1)–C(2)	1.683(11)	P(2)–C(2)	1.815(10)
P(2)–C(1)	1.873(11)	P(3)–C(12)	1.843(11)
P(3)–C(1)	1.906(10)	P(4)–C(12)	1.702(11)
P(4)–C(11)	1.848(11)	C(1)–C(3)	1.597(14)
C(2)–C(7)	1.54(2)	C(11)–C(13)	1.561(14)
C(12)–C(17)	1.523(14)		
C(1)–Sb(1)–C(11)	88.9(4)	C(1)–Sb(1)–P(1)	89.7(3)
C(11)–Sb(1)–P(1)	99.9(3)	C(11)–Sb(2)–P(3)	84.5(3)
C(11)–Sb(2)–P(2)	97.4(3)	P(3)–Sb(2)–P(2)	70.13(10)
C(11)–Sb(2)–W(2)	138.3(3)	P(3)–Sb(2)–W(2)	122.75(7)
P(2)–Sb(2)–W(2)	120.30(7)	C(2)–P(1)–W(1)	140.8(4)
C(2)–P(1)–Sb(1)	101.6(4)	W(1)–P(1)–Sb(1)	117.44(12)
C(2)–P(2)–C(1)	109.4(5)	C(2)–P(2)–Sb(2)	107.0(3)
C(1)–P(2)–Sb(2)	83.2(3)	C(12)–P(3)–C(1)	109.6(5)
C(12)–P(3)–Sb(2)	93.8(3)	C(1)–P(3)–Sb(2)	82.8(3)
C(12)–P(4)–C(11)	104.6(5)	C(3)–C(1)–P(2)	113.2(7)
C(3)–C(1)–P(3)	114.3(7)	P(2)–C(1)–P(3)	99.1(5)
C(3)–C(1)–Sb(1)	111.0(7)	P(2)–C(1)–Sb(1)	107.0(5)
P(3)–C(1)–Sb(1)	111.6(5)	C(7)–C(2)–P(1)	126.2(8)
C(7)–C(2)–P(2)	112.8(8)	P(1)–C(2)–P(2)	121.0(6)
C(13)–C(11)–P(4)	112.3(7)	C(13)–C(11)–Sb(2)	115.1(7)
P(4)–C(11)–Sb(2)	107.2(5)	C(13)–C(11)–Sb(1)	116.7(7)
P(4)–C(11)–Sb(1)	95.8(4)	Sb(2)–C(11)–Sb(1)	107.8(4)
C(17)–C(12)–P(4)	118.9(8)	C(17)–C(12)–P(3)	117.9(8)
P(4)–C(12)–P(3)	122.6(6)		

all similar and exhibit four inequivalent *tert*-butyl resonances that are significantly broadened. This broadening has been attributed to a restricted rotation of these groups due to their proximity to bulky $M(CO)_5$ fragments. Finally, the infrared spectra of **3–5** confirm the presence of ligated $M(CO)_5$ fragments.

The molecular structures of compounds **3–5** are isomorphous and so only that for **3** is shown in Fig. 1, though selected bond lengths and angles for all compounds are collected in Tables 1–3. The structures reveal that the framework of the cage starting material has remained intact and that $M(CO)_5$ fragments are co-ordinated in an η^1 fashion to P(1) and Sb(2). It is perhaps surprising that one $M(CO)_5$ fragment is preferentially co-ordinated by an Sb instead of one of the three unco-ordinated P centres. The reason for this is no doubt steric in

origin as P(2), P(3) and P(4) are bonded on either side to two bulky C₄H₉ fragments. The P(1)–M(1) distances in **3–5** all lie in the normal regions as do the Sb(2)–M(2) bond lengths {*cf.* 2.625 Å in [Sb₂Ph₄{Cr(CO)₅}₂];⁸ 2.756 Å in [Mo(CO)₅(SbPh₃)] and 2.754 Å in [W(CO)₅(SbPh₃)]⁹. All bond lengths within the framework of the cage ligands in **3–5** are consistent with single bonded interactions except those for P(1)–C(2) and P(4)–C(12) which are typical for localized P–C double bonds. As in **1** complexes **3–5** contain very strained diphosphastibacyclobutane fragments, Sb(2)P(3)C(1)P(2), in which the cross ring P⋯P distances (**3** 2.883, **4** 2.871, **5** 2.877; *cf.* 2.822 Å in **1**) are well within the sum of the van der Waals radii, 3.8 Å, for two phosphorus atoms. These close contacts could explain the large two bond PP couplings between P(2) and P(3) in the ³¹P-¹H NMR spectra of these complexes.

The reactions of compound **1** with a number of other transition metal carbonyl complexes, *e.g.* [Fe₂(CO)₉], were investigated but this generally led to decomposition of the cage compound to an intractable mixture of products. However, some success was achieved with the reaction of **1** with four equivalents of [Fe₂(CO)₉] in hexane at room temperature. This led to the isolation of **6** in moderate yield (33%) after column chromatography (Kieselgel, hexane–diethyl ether 10:1) (Scheme 2). Compound **6** is a red crystalline solid that is



Scheme 2 Reagents and conditions: i, [Fe₂(CO)₉], hexane, 18 h; ii, –CO.

thermally stable in the solid state (decomp. 160 °C) but slowly decomposes in solution over 3 d.

It seems likely that the formation of compound **6** proceeds *via* the initial formation of a 3:1 adduct, **7**, though no evidence for such a complex was seen in the NMR spectra of the product mixture, even if the reaction was stopped after one hour. If this is the case, **7** could rearrange *via* the insertion of an iron carbonyl fragment into the Sb(2)–P(3) bond (see Fig. 2) to give **6** with a concomitant loss of one carbonyl ligand. Similar insertions of transition metal carbonyl fragments into Group 15–Group 15 bonds have been reported in the formation of Group 15–transition metal clusters.^{3a,b} The iron centre in the Fe(CO)₃ fragment of **6** is best described as being σ bonded to an antimonide fragment and η³ bonded to a 1,3-diphosphaallyl system. It is noteworthy that 1,3-diphosphaallyl complexes have been previously reported¹⁰ and, in particular, those involving η³ co-ordination to a Fe(CO)₃ unit are known.¹¹ It is also interesting that the cage rearrangement that led to the formation of **2**

Table 4 Selected intramolecular distances (Å) and angles (°) for compound **6** with e.s.d.s in parentheses

Sb(1)–C(1)	2.23(2)	Sb(1)–C(11)	2.28(2)
Sb(1)–P(1)	2.554(5)	Sb(2)–C(11)	2.19(2)
Sb(2)–P(2)	2.529(5)	Sb(2)–Fe(2)	2.546(3)
Sb(2)–Fe(1)	2.642(3)	Fe(1)–P(3)	2.370(6)
Fe(1)–P(4)	2.443(5)	Fe(3)–P(1)	2.213(6)
P(1)–C(2)	1.70(2)	P(2)–C(1)	1.85(2)
P(2)–C(2)	1.89(2)	P(3)–C(12)	1.85(2)
P(3)–C(1)	1.92(2)	P(4)–C(12)	1.71(2)
P(4)–C(11)	1.88(2)		
C(1)–Sb(1)–C(11)	94.8(6)	C(1)–Sb(1)–P(1)	86.1(5)
C(11)–Sb(1)–P(1)	96.9(4)	C(11)–Sb(2)–P(2)	99.7(5)
C(11)–Sb(2)–Fe(2)	126.9(4)	P(2)–Sb(2)–Fe(2)	117.63(13)
C(11)–Sb(2)–Fe(1)	87.6(5)	P(2)–Sb(2)–Fe(1)	95.05(14)
Fe(2)–Sb(2)–Fe(1)	122.25(11)	C(23)–Fe(1)–P(3)	91.9(6)
C(22)–Fe(1)–P(3)	93.6(7)	C(21)–Fe(1)–P(3)	167.7(6)
C(12)–Fe(1)–P(3)	47.4(4)	C(23)–Fe(1)–P(4)	153.7(6)
C(22)–Fe(1)–P(4)	116.2(6)	C(21)–Fe(1)–P(4)	85.6(6)
C(12)–Fe(1)–P(4)	42.6(4)	P(3)–Fe(1)–P(4)	82.4(6)
C(22)–Fe(1)–Sb(2)	170.9(6)	C(21)–Fe(1)–Sb(2)	89.5(6)
C(12)–Fe(1)–Sb(2)	97.2(5)	P(3)–P(1)–Sb(2)	89.6(2)
P(4)–Fe(1)–Sb(2)	72.7(2)	C(2)–P(1)–Fe(3)	134.5(7)
C(2)–P(1)–Sb(1)	105.1(7)	Fe(3)–P(1)–Sb(1)	119.3(2)
C(1)–P(2)–C(2)	106.5(8)	C(1)–P(2)–Sb(2)	95.3(5)
C(2)–P(2)–Sb(2)	100.4(5)	C(12)–P(3)–C(1)	110.1(7)
C(12)–P(3)–Fe(1)	62.2(5)	C(1)–P(3)–Fe(1)	114.4(5)
C(12)–P(4)–C(11)	112.4(8)	C(12)–P(4)–Fe(1)	61.9(6)
C(11)–P(4)–Fe(1)	101.4(5)	P(2)–C(1)–P(3)	109.8(9)
P(2)–C(1)–Sb(1)	107.8(7)	P(3)–C(1)–Sb(1)	108.7(7)
P(1)–C(2)–P(2)	116.6(10)	P(4)–C(11)–Sb(2)	95.4(8)
P(4)–C(11)–Sb(1)	104.6(7)	Sb(2)–C(11)–Sb(1)	107.1(6)
P(4)–C(12)–P(3)	125.8(10)	P(4)–C(12)–Fe(1)	75.5(6)
P(3)–C(12)–Fe(1)	70.4(5)		

was thought to occur *via* cleavage of the other Sb–P bond in the strained four-membered SbPCP ring in the cage ligand.⁵

The spectroscopic data for compound **6** support its proposed structure. Its ³¹P-¹H NMR spectrum displays a signal at low field (δ 300.5) which has been assigned to the phosphorus centre involved in the localized P(1)–C(2) double bond. The signals for P(3) and P(4) (δ 107.3 and 122.4) are in the normal region for η³ co-ordinated 1,3-diphosphaallyl systems, though the ²J_{P(3)P(4)} coupling of 10 Hz is low for such systems. Also unusual is the relatively low field resonance for the saturated phosphorus centre P(2) at δ 94.4 which can be compared to a value of δ –18.6 for the same phosphorus in the cage, **1**,⁴ prior to rearrangement. As expected the ¹H NMR spectrum of **6** exhibits four broad singlets for the four inequivalent, rotationally hindered *tert*-butyl groups.

Compound **6** crystallizes with two crystallographically independent molecules in the asymmetric unit that are geometrically very similar. As a result the molecular structure of only one of these is depicted in Fig. 2 (see also Table 4) and confirms that the cage framework of the starting material has rearranged to include one Fe(CO)₃ fragment within the cage structure and two η¹-ligated Fe(CO)₄ fragments. The P(1)–Fe(3) and Sb(2)–Fe(2) distances [2.213(6) and 2.546(3) Å respectively] are in the normal region for such interactions {*cf.* 2.239 Å in [Fe(CO)₄(PPh₂H)]¹² and 2.547 Å in [Fe(CO)₄(SbBu^t₃)]¹³. The iron–antimonide bond length, Sb(2)–Fe(1) 2.642(3) Å, is considerably longer than the Sb(2)–Fe(2) interaction but still in the typical range. The P(1)–C(2) bond length, 1.70(2) Å, is also in the normal range for localized P–C double bonds. An inspection of the P(3)–C(12)–P(4) allyl fragment reveals that it is η³ co-ordinated to the Fe(CO)₃ fragment [Fe(1)–P(4)–C(12) 61.9(6), Fe(1)–P(3)–C(12) 62.2(5)°] but in a rather unsymmetrical fashion with significant differences in the P(3)–Fe(1) [2.370(6) Å] and P(4)–Fe(1) [2.443(5) Å] bond lengths. These combined with the iron–allyl carbon bond length [Fe(1)–C(12) 2.23(2) Å] are longer than in similar systems, *e.g.* [Fe(CO)₃-{η³-Mes*PC(H)PMes*[Ni(η⁵-C₅H₅)]}] (Mes* = C₆H₂Bu^t₃-2,4,6)

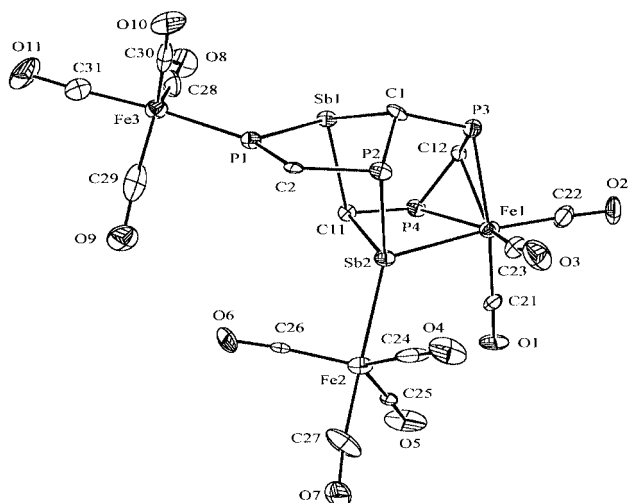


Fig. 2 Molecular structure of compound **6** (*tert*-butyl groups omitted for clarity).

[P–Fe 2.309 average, Fe–C (allyl) 2.025(7) Å¹¹]. In addition, there appears to be little delocalization over the P(3)–C(12)–P(4) fragment in **6** with the bond lengths P(3)–C(12) [1.85(2) Å] and P(4)–C(12) [1.71(2) Å] being close to what would be expected for single and double P–C bonds respectively. However, the inaccuracy in these bond lengths makes it difficult to be certain of the degree of delocalization in this system. The unsymmetrical nature of the bonding in the co-ordinated diphosphaallylic fragment can perhaps be explained by the strain present in that part of the molecule which forces the C(1) and C(11) atoms considerably out of the plane of the PCP unit. Moreover, the low ²J_{P(3)P(4)} coupling observed in the ³¹P–{¹H} NMR spectrum of **6** is consistent with the lone pairs of P(3) and P(4) being constrained to the *exo* positions of the diphosphaallylic fragment by the nature of the cage framework.

Conclusion

This study highlights the versatility of the antimony containing cage compound **1** as a ligand in the formation of transition metal carbonyl adducts **3–5**. In addition the presence of relatively weak and strained Sb–P bonds within **1** can allow its rearrangement *via* Sb–P bond cleavage upon metal coordination to afford the novel iron containing cage compound **6**.

Experimental

General remarks

All manipulations were carried out using standard Schlenk and glove-box techniques under an atmosphere of high purity argon or dinitrogen. The solvents tetrahydrofuran (THF) and hexane were distilled over Na/K alloy then freeze/thaw degassed prior to use. Dichloromethane was distilled from CaH₂ prior to use. The ¹H, ¹³C and ³¹P NMR spectra were recorded on either a Bruker WM-250 or AM 400 spectrometer in C₆D₆ and referenced to the residual ¹H resonances of the solvent used (¹H) or to external 85% H₃PO₄, δ 0.0 (³¹P). FAB Mass spectra were recorded using a VG-autospec instrument (Cs⁺ ions, 25 kV, 3-nitrobenzyl alcohol matrix). Melting points were determined in sealed glass capillaries under argon, and are uncorrected. Reproducible elemental analyses of all compounds could not be obtained due to their slight light sensitivity. However, NMR data of freshly purified samples suggested high purity of the bulk materials. The starting materials [M(CO)₅(THF)] (M = Cr, Mo or W) were generated by UV irradiation of THF solutions of [M(CO)₆] for 8 h at ambient temperature and used in solution without further purification. Compound **1** was prepared

by a published procedure.⁴ All other reagents were used as received.

Syntheses

[{Cr(CO)₅}₂(η¹:η¹-P₄Sb₂C₄Bu^t₄)] **3.** A solution of compound **1** (0.125 g, 0.19 mmol) in THF (10 ml) was added to a solution of [Cr(CO)₅(THF)] (0.11 g, 0.5 mmol) in THF (75 ml) at ambient temperature and stirred for 18 h. Volatiles were removed *in vacuo* and the residue was extracted with hexane. Purification by column chromatography (Kieselgel, hexane) and recrystallization from diethyl ether afforded **3** as red crystals (0.05 g, 24%), mp 170 °C. ¹H NMR (250 MHz, C₆D₆, 298 K): δ 1.13 (br), 1.30 (br), 1.52 (br) and 1.55 (br) (4 × 9 H Bu^t). ³¹P–{¹H} NMR (101.2 MHz, C₆D₆, 298 K): δ –16.0 [dd, P(2), ²J(P¹P²) = 25, ²J(P²P³) = 148], 31.2 [dd, P(3), ²J(P³P⁴) = 24, ²J(P²P³) = 148], 328.5 [d, P(1), ²J(P¹P²) = 25] and 355.4 [d, P(4), ²J(P³P⁴) = 24 Hz]. IR (Nujol): $\tilde{\nu}/\text{cm}^{-1}$ 2058.1s, 1960.4w, 1946.2s and 1927.7s. FAB mass spectrum: *m/z* 888 ([M – 5 CO]⁺, 9), 748 ([M – 10 CO]⁺, 17), 696 ([M – 5 CO – Cr(CO)₅]⁺, 100) and 644 ([M – 2 Cr(CO)₅]⁺, 33%).

[{Mo(CO)₅}₂(η¹:η¹-P₄Sb₂C₄Bu^t₄)] **4.** A solution of compound **1** (0.125 g, 0.19 mmol) in THF (10 ml) was added to a solution of [Mo(CO)₅(THF)] (0.13 g, 0.5 mmol) in THF (75 ml) at ambient temperature and stirred for 18 h. Volatiles were removed *in vacuo* and the residue was extracted with hexane. Purification by column chromatography (Kieselgel, hexane) and recrystallization from diethyl ether afforded **4** as red crystals (0.06 g, 29%), mp 159 °C (decomp.). ¹H NMR (250 MHz, C₆D₆, 298 K): δ 1.14 (br), 1.30 (br), 1.55 (br) and 1.61 (br) (4 × 9 H Bu^t). ³¹P–{¹H} NMR (101.2 MHz, C₆D₆, 298 K): δ –30.4 [dd, P(2), ²J(P¹P²) = 23, ²J(P²P³) = 147], 43.0 [dd, P(3), ²J(P³P⁴) = 27, ²J(P²P³) = 147], 307.7 [d, P(1), ²J(P¹P²) = 23] and 346.3 [d, P(4), ²J(P³P⁴) = 27]. IR (Nujol) $\tilde{\nu}/\text{cm}^{-1}$ 2070m, 1948.5s and 1929.1s. FAB mass spectrum: *m/z* 1115 (M⁺, 5), 881([M + H – Mo(CO)₅]⁺, 13) and 644 ([M + H – 2 Mo(CO)₅]⁺, 100%).

[{W(CO)₅}₂(η¹:η¹-P₄Sb₂C₄Bu^t₄)] **5.** A solution of compound **1** (0.15 g, 0.23 mmol) in THF (10 ml) was added to a solution of [W(CO)₅(THF)] (0.23 g, 0.58 mmol) in THF (75 ml) at ambient temperature and stirred for 18 h. Volatiles were removed *in vacuo* and the residue was extracted with diethyl ether. Recrystallization from dichloromethane afforded **5** as red crystals (0.08 g, 27%), mp 175 °C (decomp.). ¹H NMR (250 MHz, C₆D₆, 298 K): δ 1.28 (br), 1.33 (br), 1.35 (br) and 1.36 (br) (4 × 9 H, Bu^t). ³¹P–{¹H} NMR (101.2 MHz, C₆D₆, 298 K): δ –32.0 [dd, P(2), ²J(P¹P²) = 22, ²J(P²P³) = 148], 43.6 [dd, P(3), ²J(P³P⁴) = 23, ²J(P²P³) = 148], 268.5 [d, P(1), ²J(P¹P²) = 22, ¹J_{WP} = 208] and 346.2 [d, P(4), ²J(P³P⁴) = 23 Hz]. IR (Nujol): $\tilde{\nu}/\text{cm}^{-1}$ 2068.0m, 1940.7s, and 1932.2m. FAB mass spectrum: *m/z* 1293 ([M + H]⁺, 10), 969 ([M + H – W(CO)₅]⁺, 25), and 644 ([M + H – 2 W(CO)₅]⁺, 100%).

[{Fe(CO)₄}₂{Fe(CO)₃(η³:η¹-P₄Sb₂C₄Bu^t₄)}] **6.** To a solution of compound **1** (0.125 g, 0.19 mmol) in hexane (30 ml) at ambient temperature was added [Fe₂(CO)₉] (0.27 g, 0.475 mmol) and the resulting solution stirred for 18 h. Volatiles were removed *in vacuo* and the residue was extracted with hexane. Purification by column chromatography (Kieselgel, hexane–diethyl ether 10:1) and recrystallization from hexane afforded **6** as red crystals (0.06 mg, 33%), mp 160 °C. ¹H NMR (250 MHz, C₆D₆, 278 K): δ 1.12 (br), 1.20 (br), 1.29 (br) and 1.48 (br) (4 × 9 H Bu^t). ³¹P–{¹H} NMR (101.2 MHz, C₆D₆, 298 K): δ 94.4 [dd, P(2), ²J(P²P¹) = 40, ²J(P²P³) = 41], 107.3 [d, P(4), ²J(P⁴P³) = 10], 122.4 [dd, P(3), ²J(P³P⁴) = 10, ²J(P³P²) = 40] and 300.5 [d, P(1), ²J(P¹P²) = 40 Hz]. IR (Nujol): $\tilde{\nu}/\text{cm}^{-1}$ 2036.0s, 1984.8m and 1953.6m. FAB mass spectrum: *m/z* 1119 (M⁺, 5), 979 ([M – Fe(CO)₃]⁺, 7), 812 ([M – Fe₂(CO)₇]⁺, 37) and 765 ([M – Fe₂(CO)₉]⁺, 100%).

Table 5 Crystal data for $[\{M(\text{CO})_5\}_2(\eta^1:\eta^1\text{-P}_4\text{Sb}_2\text{C}_4\text{Bu}_4^t)]$ ($M = \text{Cr}$ **3**, Mo **4** or W **5**) and $[\{\text{Fe}(\text{CO})_4\}_2\{\text{Fe}(\text{CO})_4\}_2\{\text{Fe}(\text{CO})_3(\mu^3:\eta^1\text{-P}_4\text{Sb}_2\text{C}_4\text{Bu}_4^t)\}]$ **6**

	3	4	5	6
Chemical formula	$\text{C}_{30}\text{H}_{36}\text{Cr}_2\text{O}_{10}\text{P}_4\text{Sb}_2$	$\text{C}_{30}\text{H}_{36}\text{Mo}_2\text{O}_{10}\text{P}_4\text{Sb}_2$	$\text{C}_{30}\text{H}_{36}\text{W}_2\text{O}_{10}\text{P}_4\text{Sb}_2$	$\text{C}_{31}\text{H}_{36}\text{Fe}_3\text{O}_{11}\text{P}_4\text{Sb}_2$
M	1027.97	1115.85	1291.67	1119.53
Crystal system	Monoclinic	Monoclinic	Monoclinic	Monoclinic
Space group	$P2_1/n$	$P2_1/n$	$P2_1/n$	$P2_1/n$
$a/\text{\AA}$	10.2670(10)	10.324(3)	10.314(2)	20.047(2)
$b/\text{\AA}$	22.2630(10)	22.469(2)	22.394(5)	18.059(10)
$c/\text{\AA}$	16.997(2)	17.2510(10)	17.1990(10)	22.781(6)
$\beta/^\circ$	93.060(12)	93.070(10)	93.07(2)	92.420(10)
$V/\text{\AA}^3$	3879.5(6)	3996.0(12)	3966.8(12)	8240(5)
Z	4	4	4	8
T/K	150(2)	150(2)	150(2)	150(2)
$\mu(\text{Mo-K}\alpha)/\text{cm}^{-1}$	21.38	21.59	73.38	25.33
Reflections collected	14993	14464	15179	26338
No. unique reflections	5745	5564	5757	11069
R (all data)	0.0866	0.0893	0.0695	0.1758
$[I > 2\sigma(I)]$	0.0389	0.0378	0.0336	0.0526
R' (all data)	0.0797	0.0842	0.0690	0.1152
$[I > 2\sigma(I)]$	0.0723	0.0765	0.0633	0.0903

Structure determinations

Crystals of compounds **3–6** suitable for structure determination were mounted in silicone oil. Intensity data were measured on a FAST¹⁴ area detector diffractometer using Mo-K α radiation. The structures of **4** and **5** were solved by direct methods and those of **3** and **6** by the heavy atom method (SHELXS 86¹⁵) and refined by least squares using the SHELXL 93¹⁶ program. The structures were refined on F^2 using all data. Neutral-atom complex scattering factors were employed.¹⁷ Empirical absorption corrections were carried out by the DIFABS method.¹⁸ Crystal data, details of data collections and refinement are given in Table 5. Anisotropic thermal parameters were refined for all non-hydrogen atoms. The hydrogen atoms in all structures were included in calculated positions (riding model).

CCDC reference number 186/1533.

Acknowledgements

We gratefully acknowledge financial support from EPSRC (studentship for R. C. T.).

References

- 1 K. B. Dillon, F. Mathey and J. F. Nixon, in *Phosphorus: The Carbon Copy*, Wiley, Chichester, 1998; R. Streubel, *Angew. Chem., Int. Ed. Engl.*, 1995, **34**, 436; A. Mack and M. Regitz, *Chem. Ber.*, 1997, **130**, 823 and refs. therein; G. Fritz, *Adv. Inorg. Chem.*, 1987, **31**, 171 and refs. therein.
- 2 P. B. Hitchcock, C. Jones and J. F. Nixon, *J. Chem. Soc., Chem. Commun.*, 1995, 2167; V. Caliman, P. B. Hitchcock, C. Jones and J. F. Nixon, *Phosphorus Sulfur Silicon Relat. Elem.*, 1996, **113**, 15.
- 3 (a) K. H. Whitmire, *Adv. Organomet. Chem.*, 1997, **42**, 1; (b) K. H. Whitmire, in *Chemistry of Arsenic, Antimony and Bismuth*, ed. N. C.

- Norman, Blackie Academic, London, 1998; (c) A. J. Dimaio and A. L. Rheingold, *Chem. Rev.*, 1990, **90**, 169; (d) S. P. Mattawana, K. Promrai, J. C. Fettinger and B. W. Eichhorn, *Inorg. Chem.*, 1998, **37**, 6222 and refs. therein.
- 4 S. J. Black, M. D. Francis and C. Jones, *Chem. Commun.*, 1997, 305.
- 5 S. J. Black, D. E. Hibbs, M. B. Hursthouse, C. Jones, K. M. A. Malik and R. C. Thomas, *J. Chem. Soc., Dalton Trans.*, 1997, 4321.
- 6 K. Karaghiosoff, in *Multiple Bonds and Low Co-ordination in Phosphorus Chemistry*, eds. M. Regitz and O. J. Scherer, G. Thieme, Stuttgart, 1990, pp. 463–465.
- 7 C. Elschenbroich, S. Voss, O. Schiemann, A. Lippek and K. Harms, *Organometallics*, 1998, **17**, 4417.
- 8 J. von Seyerl and G. Huttner, *Cryst. Struct. Commun.*, 1980, **9**, 1099.
- 9 M. J. Aroney, I. E. Buys, M. S. Davies and T. W. Hambley, *J. Chem. Soc., Dalton Trans.*, 1994, 2827.
- 10 R. El-Ouatib, D. B. Tkatchenko, G. E. Moghadam and M. Koenig, *J. Organomet. Chem.*, 1993, **453**, 77; R. Appel, W. Schuhn and F. Knoch, *J. Organomet. Chem.*, 1987, **319**, 345.
- 11 H. Schmidbaur, W. Graf and G. Müller, *Angew. Chem., Int. Ed. Engl.*, 1988, **27**, 417.
- 12 B. T. Kilbourn, V. A. Raeburn and D. T. Thompson, *J. Chem. Soc. A*, 1969, 1906.
- 13 A. L. Rheingold and M. E. Fountain, *Acta Crystallogr., Sect. C*, 1985, **41**, 1162.
- 14 J. A. Darr, S. A. Drake, M. B. Hursthouse and K. M. A. Malik, *Inorg. Chem.*, 1993, **32**, 5704.
- 15 G. M. Sheldrick, *Acta Crystallogr., Sect. A*, 1990, **46**, 467.
- 16 G. M. Sheldrick, SHELXL 93, Program for Crystal Structure Refinement, University of Göttingen, 1993.
- 17 *International Tables for X-Ray Crystallography*, eds. J. A. Ibers and W. C. Hamilton, Kynoch Press, Birmingham, 1974, vol. 4.
- 18 N. P. C. Walker and D. Stuart, *Acta Crystallogr., Sect. A*, 1983, **39**, 158; adapted for FAST geometry by A. I. Karavlov, University of Wales, Cardiff, 1991.

Paper 9/03136C